22nd ITS World Congress, Bordeaux, France, 5–9 October 2015

Paper number ITS-2492

Positioning Accuracy of Vehicle Trajectories for Road Applications

P. Clausen[1], P-Y. Gilliéron[1*]
H. Perakis[2], V. Gikas[2], I. Spyropoulou[2]
1. École Polytechnique Fédérale de Lausanne, Switzerland
*EPFL ENAC IIE TOPO, GC C2 398 (Bâtiment GC), Station 18, CH-1015 Lausanne;
+41 21 69 32750; pierre-yves.gillieron@epfl.ch;
2. National Technical University of Athens, Greece

Abstract
Global Navigation Satellite Systems (GNSS) has become a kind of positioning standard due to the high penetration rate of this technology on mass market ITS applications. However, this positioning technique remains a real challenge for very demanding services. This paper reports on a practical and methodological approach for the evaluation of the GNSS positioning and attitude of vehicles in real life conditions. Test scenarios have been set up with several positioning sensors mounted on a vehicle for the collection of raw data on different road sections. The measurement of a high quality reference trajectory allowed to estimate position accuracy under different environmental conditions. We will show in detail the results and identify some typical situations where the quality of GNSS-only positioning is reduced and may impact the level of ITS services, e.g. road user charging or safety applications.

Keywords: GNSS, positioning accuracy, SaPPART

1 Introduction

Despite the broad usage of GNSS technology for most outdoor positional, navigational and timing activities there are cases where the reliance on satellite navigation systems cannot be guaranteed due to degraded data quality or intermittent signal reception. Specifically, in the road environment, satellite signal blockage caused by buildings and steep gradients, signal attenuation due to tree canopy as well as interference owing to passing traffic such as vehicles and pedestrians could lead to sections of limited satellite availability and degraded signal quality resulting in a poor navigation solution (Danezis and Gikas, 2013). Evidently, such a deteriorated navigation solution has a profound effect on most ITS applications that

necessitate reliable location information of all elements of a transportation network (Retscher and Kealy, 2006). Today, GNSS data is broadly used in navigation systems, e.g. provision of real time information systems for buses. Such systems require vehicle positioning, however, data accuracy is not critical.

In ITS where data accuracy is critical, other types of technologies are used - usually optical-based sensors embedded in the vehicle. Advanced driver assistance systems (ADAS) that provide support to the driver to prevent a crash is only one example (pre-crash systems). Another example is lane departure warning (LDW), where part of the system operation is as follows: a sensor identifies lane markings on the pavement and warnings are triggered if a lane departure is monitored. System accuracy depends greatly on the quality of lane markings and on specific prevailing conditions including weather, lighting and pavement. In particular frost, snow, low temperatures, oncoming headlights or low sun deteriorate the system performance. In addition, a sensor based systems increases the cost of the product.

Another typical category of ITS, where GNSS could allow improved and quicker implementation of ITS systems, is “cooperative ITS” where the system involves vehicle-to-vehicle communication. In such cases high penetration rates are required to be effective. GNSS based systems can fulfil this criteria. Such systems range from simple systems that communicate real time information (e.g. an incident while en-route is identified and this information is transmitted to relevant other vehicles) to more complex ones such as vehicle collision warnings or even fully automated highway systems (AHS). Last, there is another family of systems, which can only operate with continuous positioning such as e-call and road user charging (RUC). The latter can operate with limited payment strategies using a manifold of different infrastructure technologies (cameras/toll stations in allocated locations).

To improve stand-alone GNSS performance, various low-cost products have been proposed recently to facilitate the end user’s localization needs encountered in the road sector. Such systems rely either on specialized data processing algorithms, external sensor (e.g. accelerometers, gyroscopes, odometer and magnetometer) and cameras or even on communication network-assisted GNSS principles (Groves, 2012). Depending on the specific application needs, low-cost vehicle localization systems operate as external devices or they form part of the vehicle motion control system in modern cars. However, as these systems are still new and mostly at a prototype level, testing of their performance is required, especially at GNSS signal challenged situations such as in the urban environment (Stebler et al, 2011).

ITS services are rapidly growing with an increased number of location-based applications. Due to the requirements of such advanced applications, several initiatives have been initiated for the development of standards and the definition of quality metrics in GNSS based positioning. This activity requires a high level coordination between the GNSS actors, the automotive industry and the ITS service providers. The SaPPART (*Satellite Positioning Performance Assessment for Road Applications*) COST Action TU1302 (Gilliéron and Peyret, 2014) has been introduced to improve cooperation between the ITS and GNSS communities.

This article is the product of a short term scientific mission undertaken within the frame of SaPPART between the École Polytechnique Fédérale de Lausanne in Switzerland (EPFL) and the National Technical University of Athens in Greece (NTUA). It presents preliminary results of an experimental work which aims to assess the performance of a number of GNSS receivers in variable satellite signal reception conditions. More specifically, the main focus of the paper is to undertake a series of thoroughly designed field tests, compute suitable positional accuracy features for the GNSS-only solutions and compare them against a reference trajectory obtained using a high-end GNSS/INS system and specialized processing techniques (Waegli et al, 2008). The goal of this work is to contribute in the characterization of kinematic GNSS error sources and to study their impact on vehicle positioning accuracy for ITS applications. The output of this experiment is composed of a data set which will contribute to the development of a methodology for the assessment of positioning terminal performance. In addition, a preliminary evaluation of the potential of contemporary smartphone navigation sensors is attempted. However, the study of GNSS position availability, protection levels and integrity performance would go out of the scope of this work.

2 Characterization of Vehicle Trajectory Accuracy

Two statistical features are used to describe the positioning accuracy of a moving vehicle; specifically, the precision and trueness of its location and velocity estimates. Precision characterizes the performance of a vehicle navigation system that relies solely on its own error estimates and refers to the repeatability or reproducibility level of measurements. Whereas trueness of a vehicle trajectory expresses the proximity of the navigation solution to the actual (true) trajectory (ISO 5725-1, 1994). In this context, the term *accuracy* will relate to a combinatory use of the two terms *precision* and *trueness*. In statistical terms, the "dispersion" of the error probability distribution of a positioning terminal reflects its precision capability, whereas its "mean" indicates the deviation from the true trajectory and is associated to the positioning trueness or reliability of the system (see Fig. 1).

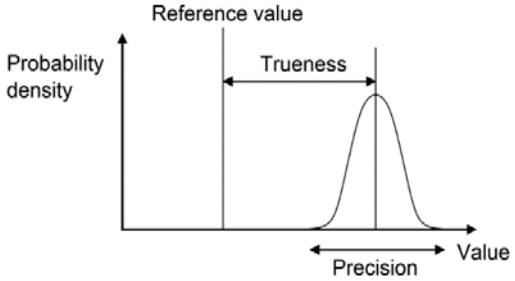

Figure 1: Vehicle positioning accuracy metrics definition [Ref: ISO 5725-1].

For navigation and ITS related applications it is essential to transform originally derived accuracy figures from a global coordinate system (e.g. eastings, northings) to their along-track and off-track equivalents. This is done in order to produce meaningful positioning accuracy

metrics. This error representation adheres to the motion characteristics and therefore facilitates the means to control and asses the longitudinal and lateral vehicle kinematics.
In order to compute along-track and off-track precision measures, an estimate of the running vehicle steerage (heading) is needed. This allows to convert positioning errors from a cartographic coordinate system to a local level coordinate system with the vehicle placed in the centre (see Fig. 2, left). On the contrary, in order to assess the trueness of a navigation solution, a reference trajectory is required against which a comparison is made to. In this case, the along- and off-track accuracy of an observed travel path reflects its deviation from the ground truth (see Fig. 2, right). Specifically, the along-track error allows to represent the error in the direction of movement between the calculated position and the reference trajectory whereas the off-track error expresses the lateral offset of the calculated position from the ground truth.

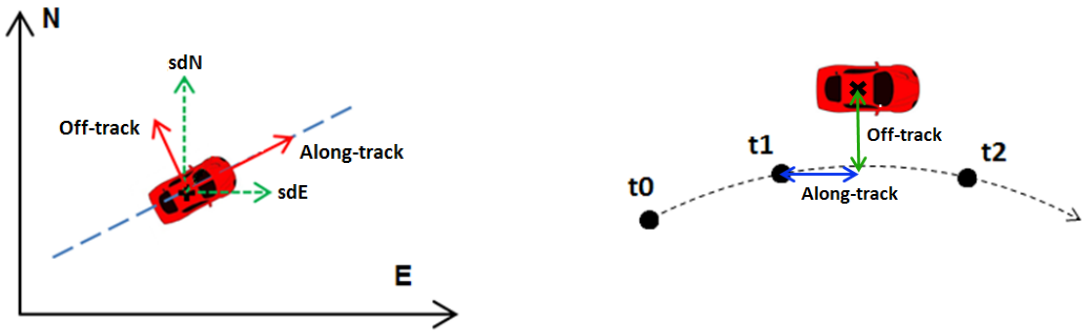

Figure 2: Left: Schematic view of the precision. The global precision estimates in East (sdE) and North (sdN) direction are projected to their along- and off-track equivalents; Right: Schematic view of the trueness. The position is compared to the reference trajectory at specific timestamps.

Extracted vehicle trajectories solely based on a geodetic-grade GNSS post-processed kinematic (PPK) solution may facilitate a viable option in terms of accuracy; however, they might suffer by lower continuity and availability statistics compared to the coarse (code-only) GNSS solution. The integration of a geodetic grade GNSS receiver with a high-end inertial navigation system (INS) offers today the most widely accepted way to establish a high quality vehicle trajectory (Kealy *et al*, 2012; Musoff and Zarchan, 2005). In fact, the complementary properties of the two systems make them ideal partners, as the long-term accuracy of the GNSS bounds the drifts of the INS, whereas the INS can bridge the gaps in the GNSS positioning resulting from signal blockage (e.g. due to buildings or tree canopies). Moreover, the high operation frequency of the INS will even enable to close the gaps between the low-frequency position fixes of the GNSS. Table 1 summarizes the complementarity of these two systems. Depending on the GNSS receiver, the INS sensor characteristics, the processing technique, and environmental conditions a precision accuracy in the centimetre level can be expected. The processing technique adopted here is discussed later on in detail in Section 4.

Table 1: Complementarity between a GNSS and an INS systems.

Characteristic	GNSS	INS
Information	Absolute	Relative
Output rate	Low	High
Short term accuracy	Low	High
Long term accuracy	High	Low
Availability	Limited	Unlimited

3 Experimental Setup and Field Tests

3.1 Navigation Systems Used

Several field tests were undertaken using a multitude of vehicle positioning sensors. Specifically, three types of navigation systems were used: (a) a high-end GNSS/INS system to provide the vehicle reference trajectory, (b) a number of standalone GNSS units including a smartphone and a tablet PC, and (c) a GNSS receiver augmented by a series of redundant IMU (inertial measurement unit) sensors.

Table 2 summarizes the performance characteristics of the integrated GNSS/INS system. It composes the navigation-grade INS *Ixsea AirINS* and the geodetic-grade GNSS receiver *Javad Delta T3G* connected to a *Javad GrAnt-G3T-JS* antenna. Data logging for the *AirINS* system was performed using the *Scan2Map*™ *(*topo.epfl.ch/scan2map) acquisition unit, which also provides the power supply for the INS as well as for the GNSS receiver. The test equipment was selected on a wide range of criteria including their technical characteristics, their cost range and their accessibility to a wide range of users. Specifically, a high-sensitivity GNSS receiver (*Ublox EVK-6T*) and a mobile device (a smartphone *Iphone 5S*) were used.

Table 2: Performance characteristics of the geodetic-grade GNSS receiver Javad Delta T3G system and the Ixsea AirINS IMU.

AirINS + GNSS performance (RMS)

	RTK	PPK
Position (m)	0.15	0.15
Velocity (m/s)	0.01	0.01
Roll/Pitch (deg)	0.005	0.0025
True heading (deg)	0.01	0.005

IMU performance

Gyroscope Drift	< 0.01 °/hr
Gyroscope Noise	< 0.0015 °/sqrt(hr)
Accelerometer Drift	< 100 µg
Acquisition Freq	200 Hz
Weight	4.5 kg
Power	15 W

The smartphone is equipped with a GNSS receiver and tri-axial inertial measurement units (accelerometers, gyroscopes and magnetometers) that could serve for the identification of driving patterns related to certain driving events. The *Ublox* receiver is a single frequency (L1-only) high-sensitivity GNSS unit featuring increased capabilities even in GNSS

challenging conditions (e.g. tree canopies and urban environment).

For the purpose of this field test, analysis is confined solely on the navigation solutions provided by the geodetic-grade GNSS receiver *Javad Delta T3G* and the *UbloxEVK-6T* as well as in the IMU measurements obtained by *iPhone 5S*. As for the test vehicle, the EPFL van (*VW Syncro)* was used as it facilitates adequate desk space for the scientific equipment.

3.2 Setup Configuration and Sensor Mounting

An important aspect concerning the preparation of the experiment was related to the proper setup and mounting of the sensors on the test vehicle. For this purpose, stability and safety concerns of all units were taken into account. The *AirINS* system and the *Javad* GNSS antenna were placed on a custom designed platform mounted on top of the vehicle using a roof rack. In order to minimize the impact of excessive vibrations on the sensor platform, a suspension system was used. The *Scan2Map*™ acquisition unit (providing power and all the connectivities) was placed inside the vehicle, whereas data recording was performed in real-time through a laptop-controller. The mounting platform specifically constructed for this experiment offered a stable and secure base for the mobile devices and for the *Ublox* GNSS antenna. Finally, in order to reduce all observations to the same origin the lever arms among all sensors were measured. Figure 3 shows an overview of the data acquisition system and a detailed view of the sensors setup on the roof top vehicle.

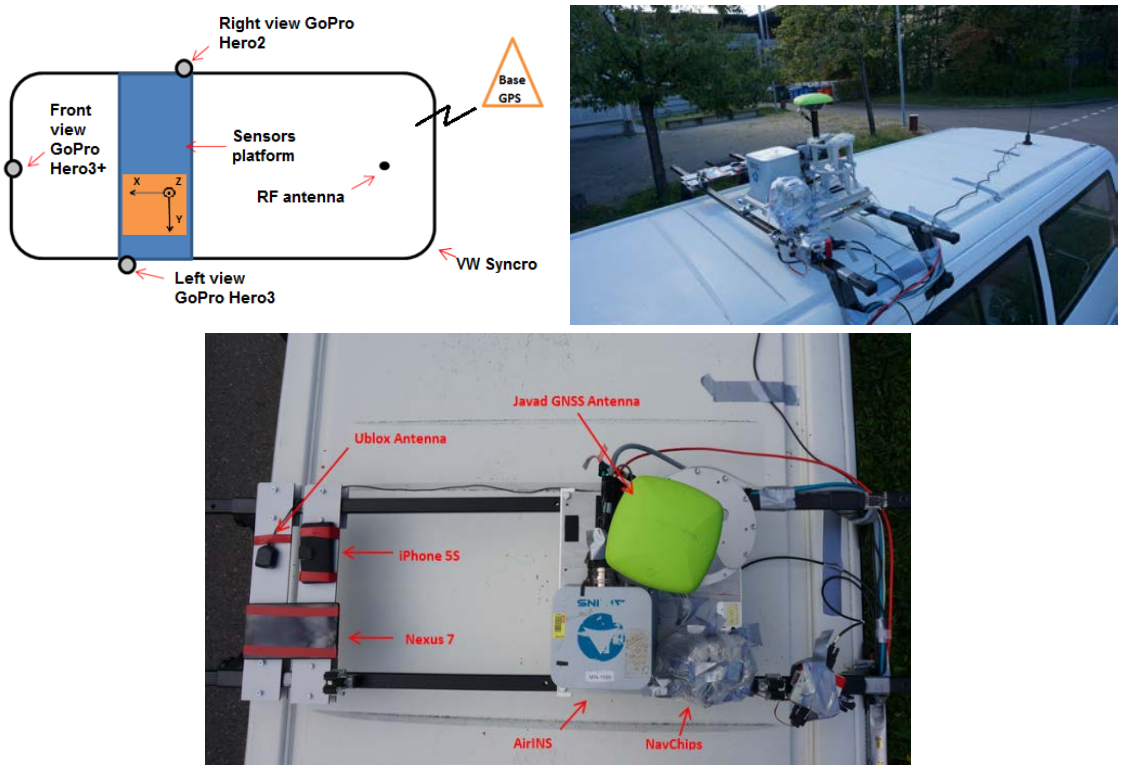

Figure 3: Navigation sensor setup overview (top-left and top-right). Detailed view of sensor platform (bottom).

3.3 Data Collection

The main field test involved the collection of vehicle navigation data along a loop-shaped travel path approximately 9.5 km long located in the Vuarrens area some 20 km North in the outskirts of Lausanne, Switzerland (see Fig. 4). The route involves parts of rural and suburban roads and an urban section towards its end characterized by relatively unfavorable satellite visibility conditions due to trees and buildings. The traveled section is flat to smooth hilly and driving speeds varied between 20 to 50 km/h.

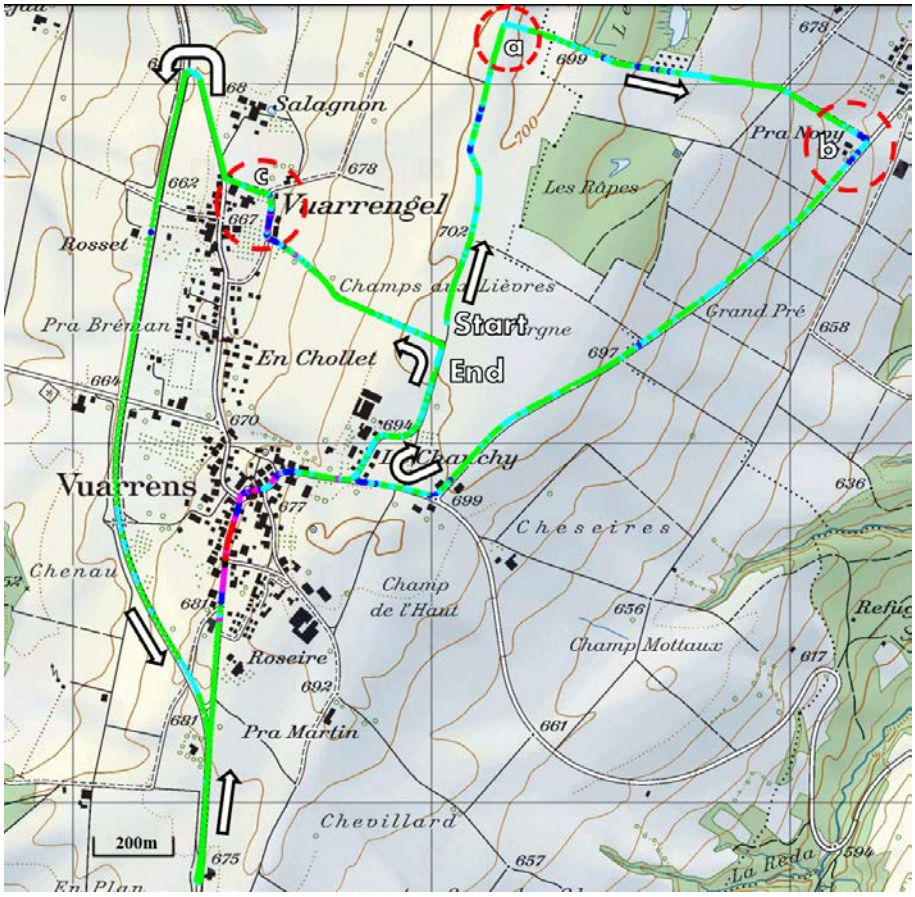

Figure 4: Travelled trajectory in Vuarrens (© 2014 swisstopo (JD100064)). Solution quality indicators in green/red. The letters a-b-c denote the places for the case studies.

Prior to data collection a pre-planning software was used (e.g. Grafnav) to select an observation time span of good satellites visibility (predicted GDOP < 3.7). During data acquisition all sensors were synchronized through the GPS pulse-per-second (PPS) signal to provide directly comparable observable data. In order to obtain a differential GNSS solution, the coordinates of a Virtual Reference Station (VRS) were acquired using the Swiss Positioning Service (www.swipos.ch) that is based on the Automated GNSS Network Switzerland (*AGNES*). This service also enables real-time positioning accuracies at the centimeter level using signal corrections for GPS and GLONASS. The required observation and correction data are made available to the mobile users by means of GSM/GPRS.

4 Measurements of Vehicle Trajectory

To establish the vehicle trajectories, the raw GNSS data were processed for each navigation system independently using a suite of software tools. Despite the ability of both systems (*Javad Delta T3G, Ublox EVK-6T)* to produce a differential solution, attention is paid on the standalone solutions. This type of solution is typically employed in the ITS sector as the receiver location is computed in an absolute sense (i.e. no differential corrections are applied) and without the need of a base station. Typical examples of this positioning technique form the low-cost handheld GNSS units embedded in smartphones and in modern automotive navigation systems. Finally, in order to allow a high fidelity accuracy assessment of the test receivers, particular attention was paid on the establishment of the reference trajectory. The next Figure 5 depicts an overview of the processing scheme used which is discussed in the following sections.

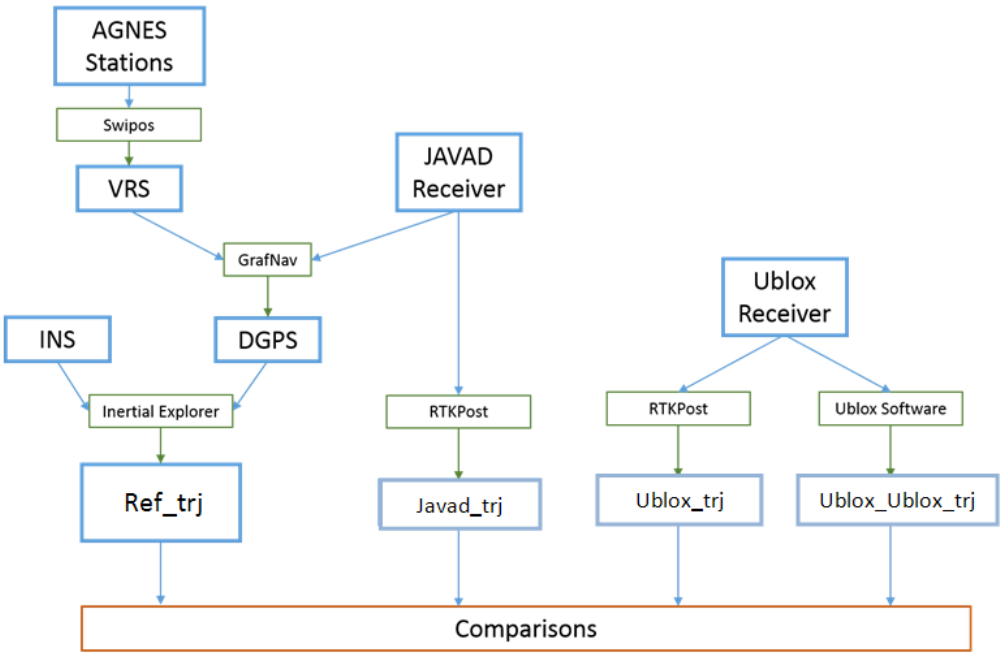

Figure 5: Data processing scheme showing the computational steps from the raw data to the final trajectories which are then compared under each other.

4.1 Establishment of Reference Trajectory

4.1.1 Processing Methodology

The establishment of the reference trajectory resulted from the fusion of GNSS and INS measurements by means of a Kalman filter that compensates the errors in their observation and kinematic stochastic models in an optimal way. Depending on the fusion level of the observation data, a Kalman filter solution grades from a loosely, to a tightly and to a deeply coupled one. In this study we use the loosely coupled filter scheme in which the GNSS and INS provide independently from each other a position-velocity-time (PVT) and position-velocity-attitude (PVA) information respectively. As shown in the left plot of Figure

6, these two are then fused into a filter and eventual corrections are re-injected to the INS processor to calibrate for drifts in the inertial measurements and finally produce an integrated solution.

To outline better the working principle of a Kalman filter the right plot of Figure 6 shows an example of a short piece of vehicle track. The GNSS coordinates (in red) are very accurate but are sampled slowly. The INS (blue points) fills the holes between the GNSS positions but progressively deviates due to its low-accuracy potential. The GNSS-position will eventually correct the INS-position and ideally calibrate the sensor errors resulting in a smoother trajectory.

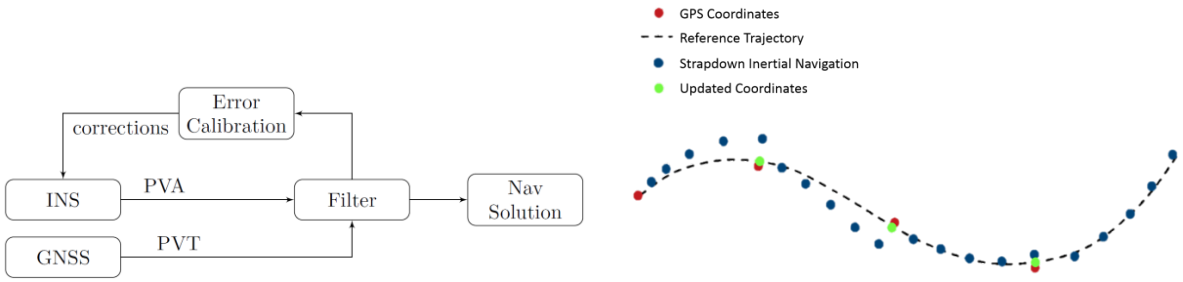

Figure 6: GNSS/INS loosely coupled integration scheme (left) and an example of a short vehicle track where GNSS and INS work together (right)

The integration of GNSS and INS data is a highly demanding computational process that requires extensive experience. The retrieval of PVA information by the INS is done through integrating the accelerations and rotations sensed by the accelerometers and gyroscopes. Special attention has to be paid to distinguish between the gravity vector and the actual acceleration the INS undergoes as wrong integration will rapidly lead to erroneous solutions (Musoff and Zarchan, 2005). The PVT of the GNSS suffers from errors too. These are manifold and consist of the errors in the satellite clocks and orbits, the effects imposed by delays though signal transmission in the troposphere/ionosphere and errors due to multipath/reflections. The majority of these errors can be handled successfully using a dual frequency receiver (to compensate for atmospheric effects) and corrections from a base station via the implementation of special processing techniques that use the complete spectrum (carrier phase and pseudorange code) of the GNSS signals. Provided that the entire process is carefully undertaken, a high positioning accuracy (cm level) can be achieved.

4.1.2 GNSS Data Processing and Fusion with INS Data

GNSS data processing is performed in accordance to the flowchart shown in Figure 5. To compute a differential GNSS solution, a virtual reference station (VRS) was used. The base station was created using the swipos-service as detailed in Section 3.3. The base station data provided by swipos were downloaded and combined with the vehicle GNSS data (*Javad Delta T3G*) using the commercial Software *Grafnaf V8.4* of *Novatel*. Figures 7 and 8 show

critical quality control features of the GNSS solution obtained by the system. The considered GPS timestamps lie between 375890 and 376880 seconds. Notably, the low quality of GNSS solution (less satellites, higher DOP values and inability to obtain a fixed solution) is evident towards the last section of the trajectory as the vehicle passes through Vuarrens village.

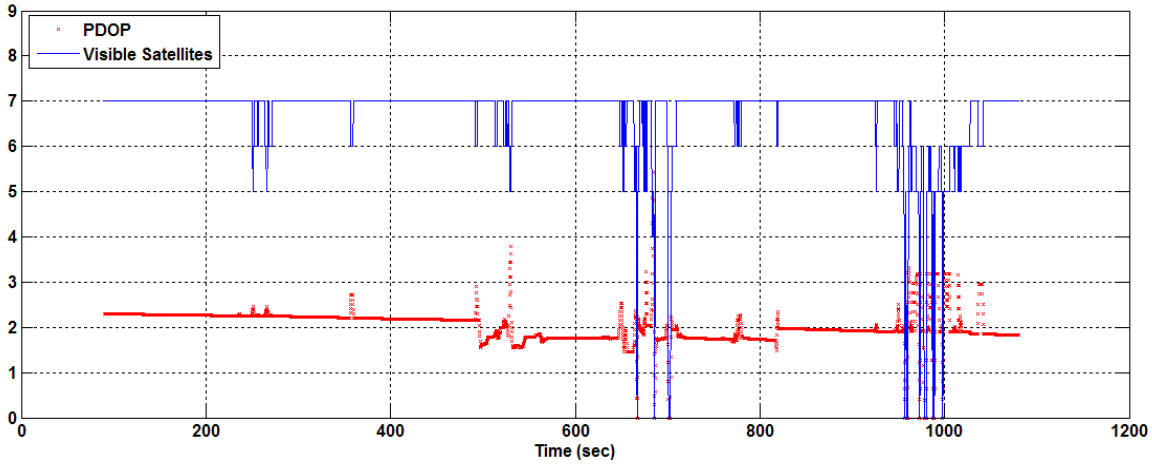

Figure 7: Number of satellites and PDOP values extracted from the data collected during the experiment. The number of satellites is generally 'good' except when moving through the village at the timestamp 1000.

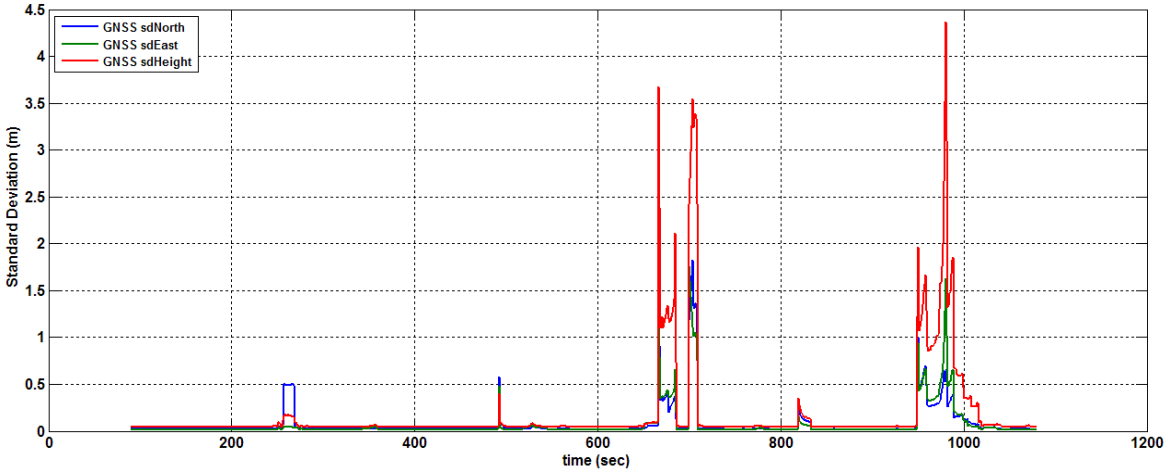

Figure 8: Estimated position standard deviation of the pure GNSS solution with the Javad receiver reaching sometimes up to several meters.

To overcome the deficiencies in the GNSS-only solution, satellite data (*Javad Delta T3G*) is co-processed with inertial data (*AirINS*) using *Novatel Inertial Explorer V8.4* software that treats the combined information through a loosely coupled Kalman filter. Prior to data processing, the lever arms (offset parameters) of the GNSS antenna with respect to the origin of the body frame were taken into account to reduce GNSS and INS measurements to a common point. Figure 4 shows the quality of the fused solution too. It uses a color representation where the color green represents an optimal solution, whereas the color red is the worst quality obtained on the trajectory.

Figure 9 shows the estimated position standard deviation of the reference trajectory as a function of time. The relatively higher error values at the end of the track are due to the deteriorated satellite visibility conditions (close to trees and in the village) which directly relates to the bad quality indicators of on Figure 4.

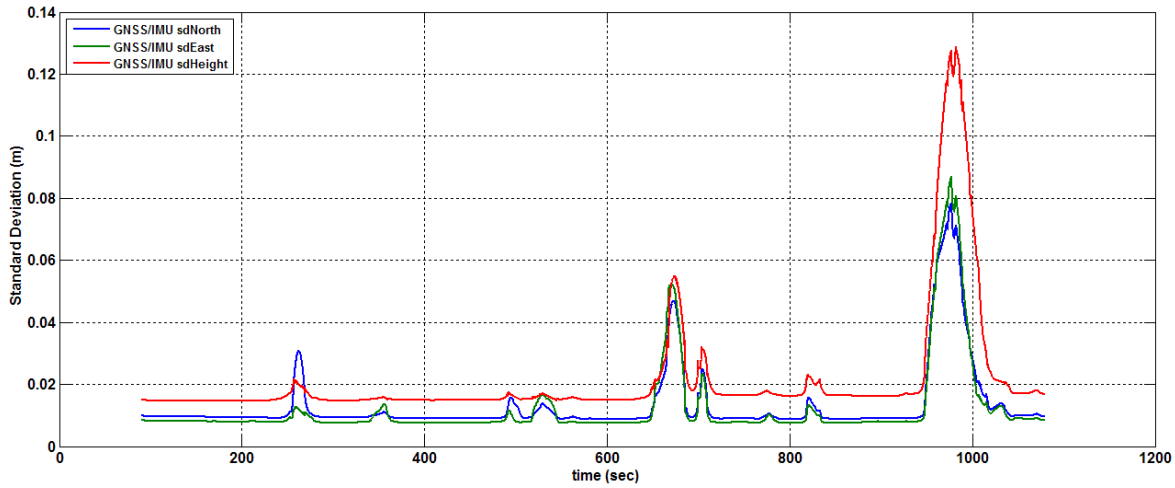

Figure 9: Estimated position standard deviation of the GNSS/INS combined and smoothed solution: the precision is mostly around 1 cm except for the village where it increases to a decimeter level.

4.2 Standalone GNSS Data Processing and Smartphone Data Extraction

4.2.1 Standalone GNSS

As already stated, the GNSS solutions of two GNSS receivers are compared in this study; namely, those for the geodetic-grade *Javad Delta T3G* and the high-sensitivity *Ublox EVK-6T* receiver. Data processing followed the procedure shown in Figure 5. Particularly, the *Javad Delta T3G* data files were converted into a *Rinex navigation file* and processed using the *RTKPost* tool of the *RTKLIB* open source software for GNSS positioning (www.rtklib.com). The solution obtained reflects the vehicle trajectory derived using only the receiver observations (i.e. no differential solution was performed) at a sampling frequency of 1 Hz. Regarding the *Ublox EVK-6T* data, in a similar manner to *Javad Delta T3G*, they were processed using *RTKPost* software to obtain the vehicle trajectory at 5 Hz and in standalone mode.

Furthermore, the *Ublox EVK-6T* data were also collected in real time using the *Ublox* proprietary software provided by the manufacturer. This solution implements some filtering/smoothing algorithms used to improve the GNSS positioning; however, the underlying assumptions and their implementation steps are unknown to the end user. The assessments of vehicle trajectories based on the comparisons between the standalone GNSS solutions and the reference trajectory are discussed in Section 5.3.

4.2.2 Smartphone Data

In this study, the analysis of the smartphone data is confined to a preliminary characterization of their navigation sensor potential to describe the vehicle kinematics. Especially, the interest is centered in situations of rapid changes in the kinematic status of the vehicle such as maneuvering/accelerating/decelerating. The data acquisition was performed using third-party software (mobile apps). Specifically, *SensorLog* application enabled the *iPHONE 5S* (iOS7) to record raw data at a sampling rate of 100 Hz. Particularly, acceleration and gyroscope data were recorded corresponding to the trajectory of movements of the vehicle.

5 Vehicle Trajectory Comparisons

This section discusses the methodological approach and the algorithmic tools developed to compute positioning accuracies of the test trajectories and attempts a critical assessment of the results obtained. As stated in Section 2, positional accuracies of vehicle trajectories are expressed in their along-track and off-track components so that they can directly be related to motion characteristics. Probably the most critical requirement to assess the accuracy estimates of a navigation solution relates to the following question: *Does the estimated position precision always keep up with the calculated position trueness (i.e. difference of the position-fix to the reference trajectory)?* Ideally, the estimated precision should be worse than the trueness in order to assure that the reference trajectory is included in a specified the sigma distance (see also Fig. 1). For instance, if someone wants to have 99.7% of the realizations within a certain boundary, one will define a 3σ boundary. The calculations done in the programs used here and the solutions on the figures are always represented as the 1σ boundary. In order to assess the accuracy potential of the observed trajectories the next two subsections present how along-track and off-track errors are computed. The proposed methodologies are distinguished for the cases of precision and trueness respectively.

5.1 Along- and Off-track Error Estimation Based on the Reference Trajectory

The position errors are calculated with respect to a reference trajectory which represents the ground truth. In the underlying process, each position fix is time-stamped with the time of week (TOW) so it is clearly defined. Besides, the sampling frequency of available position fixes is greater for the reference trajectory (10 Hz) compared to those of the test trajectories (1 Hz and 5 Hz for the *Javad Delta T3G* and the *Ublox EVK-6T* receivers respectively). This fact allows a one to one correspondence between position fixes of the observed and the reference trajectory.

The calculation of the along-track and off-track errors is made assuming a linear transition model between subsequent position fixes at times t_1 and t_2. Clearly, this simplification is valid, as no brusque maneuvers (i.e. zigzagging) are performed at high speeds, in which case would lead to a loss of eventual information associated in the space between subsequent

position fixes. According to Figure 10, a vector $\vec{a}$ is defined between two successive points of the reference trajectory resampled to the sampling frequency of the trajectory to be compared at timestamps t_1 and t_2. A second vector $\vec{b}$ is defined between the first point of the reference trajectory and the point of interest of the same timestamp t_1. The off-track error d is calculated by the scalar product (noted by $\times$), its sign and the absolute value:

$$d = \text{sign}\left(\vec{a} \times \vec{b}\right) \cdot \frac{\left|\vec{a} \times \vec{b}\right|}{\left|\vec{a}\right|} \qquad (1)$$

If the value d is positive, the point of interest lies on the left side of the trajectory, whereas a negative sign corresponds to a point location on the right site of the reference trajectory.

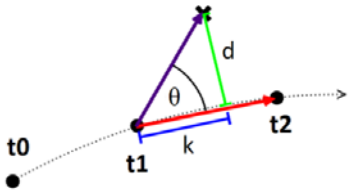

Figure 10: Calculation of the along-track (blue) and the off-track error (green) with the help of the vector a (red) and the vector b (violet) for a specific timestamp t1. The angle θ indicates the separation between those two vectors.

Subsequently, the along-track error k is calculated by taking into account the off-track error d and vector $\vec{b}$. To perform this operation, the Pythagorean Theorem is used as follows:

$$k = \sqrt{\left|\vec{b}\right|^2 - d^2} \qquad (2)$$

In order to determine the sign of the along-track error, the angle θ defined between vectors $\vec{a}$ and $\vec{b}$ is computed by the dot-product (represented with the symbol $\bullet$) using:

$$\theta = \arccos\left(\frac{\vec{a} \bullet \vec{b}}{\left|\vec{a}\right| \cdot \left|\vec{b}\right|}\right) \qquad (3)$$

For $|\theta| < \pi/2$, the point of interest lies ahead of the reference trajectory otherwise it lies behind it. Outages in the reception of the GNSS signals (e.g. due to buildings or tunnels) will lead to a loss of individual position fixes. Therefore, it may happen that for a particular timestamp there will be no position of interest. In this case, the timestamp in question is skipped and one directly proceeds to the next available point fix.

5.2 Along- and Off-track Error Estimation Based on the Pure Measurements

For each one of the standalone GNSS solutions derived for the test receivers, their along-track and off-track precision estimates is computed in two sequential steps as shown in Figure 11.

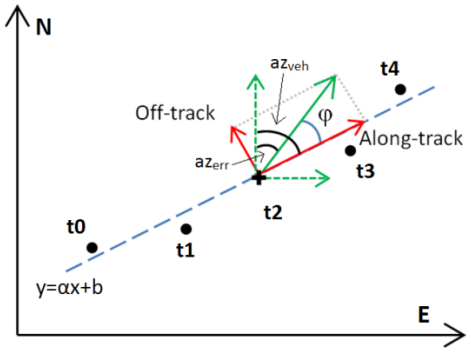

Figure 11: Definition of the along-track and off-track errors (red) given the Eastings and Northings errors (green dotted).

In the first step, for every point of interest in the observed trajectory a time window of a fixed length is defined to include *n* point fixes lying before and after the point fix in question. For this moving window a least squares fit is performed to compute the parameters *a* and *b* of the straight line that corresponds to the point fixes lying in the preset buffer length:

$$R^2(a,b) \triangleq \sum_{i=1}^{n}\left[y_i - (a + bx_i)\right]^2 \quad (4)$$

For the datasets in this study, following various sensitivity tests, a buffer length of 2.5 seconds is used given the sampling rates and noise characteristics of the navigation data.
In the second step, the running azimuth (orientation) of the moving vehicle az_{veh} is computed using the slope *a* of the straight line derived from Eq. 4. Also, the azimuth of the total precision error az_{err} is computed using the standard deviation values σ_E and σ_N respectively. Subsequently, the deviation angle φ defined between the direction of the total error vector and the direction of movement is given by:

$$\varphi = az_{veh} - az_{err} \quad (5)$$

Finally, the estimated along-track and off-track error components are computed using the angle φ and the norm of the total precision error by employing the rotation transformation:

$$\begin{aligned} \text{along\_track}_{error} &= \text{total}_{error} \cdot \cos\varphi \\ \text{off\_track}_{error} &= \text{total}_{error} \cdot \sin\varphi \end{aligned} \quad (6)$$

5.3 Results from the Field Tests

As noted in Figure 5, the accuracy features of three test trajectories are produced and evaluated. These correspond to the *Javad Delta T3G* and *Ublox EVK-6T* standalone post-processed solutions obtained using the *RTKPost* software, named "*Javad-trj*" and "*Ublox-trj*" respectively and the *Ublox EVK-6T* standalone post-processed solution obtained using the *Ublox* in-house real time solution named "*Ublox_Ublox-trj*".

Vehicle trajectory evaluation is undertaken at three levels of analyses. Firstly, we examine the influence that processing software imposes on the reliability (trueness) of a navigation solution. For this purpose we compare the along- and off-track deviations from the reference trajectory for the *Ublox-trj* and *Ublox_Ublox-trj* solutions shown in Figure 12. The first thing to note from this figure is that the *Ublox* proprietary software produces a considerably smoother track (*Ublox_Ublox-trj*) compared to the standard solution (*Ublox-trj*) obtained using an ordinary GNSS post-processing software (*RTKPost*). Evidently, it appears that the *Ublox* in-house software applies some pre-filtering algorithm to the raw GNSS data that smoothes out considerably the misplaced position fixes. However, the general accuracy trend is similar in both trajectories. The ability of *Ublox_Ublox-trj* solution to follow successfully the general pattern of the reference trajectory is further exposed in Figure 13. Particularly, this solution produces generally a robust horizontal alignment compared to the standard GNSS solution. However, given that the processing strategy behind the *Ublox_Ublox-trj* is unknown, this trajectory is not further examined.

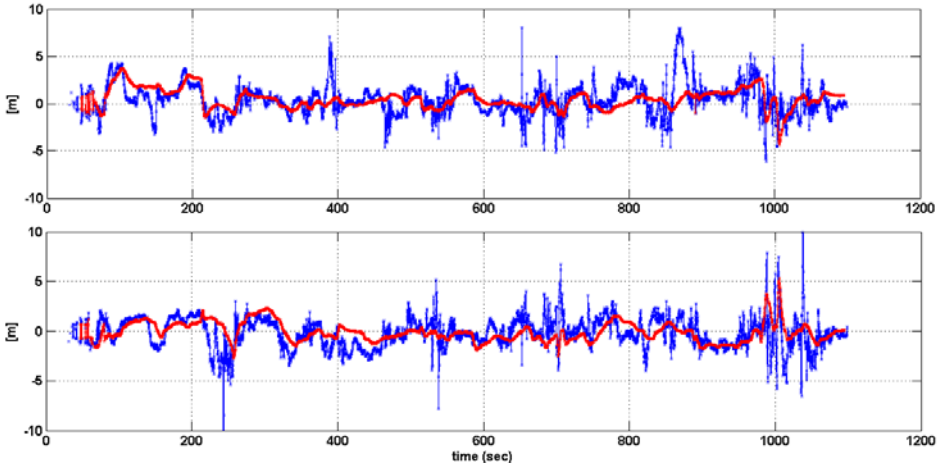

Figure 12: Cross-comparison of the error timeseries of the differences 'Ublox-trj – Ref-trj' (blue) and 'Ublox_Ublox-trj – Ref-trj' (red) in the along-track (top) and off-track directions (bottom).

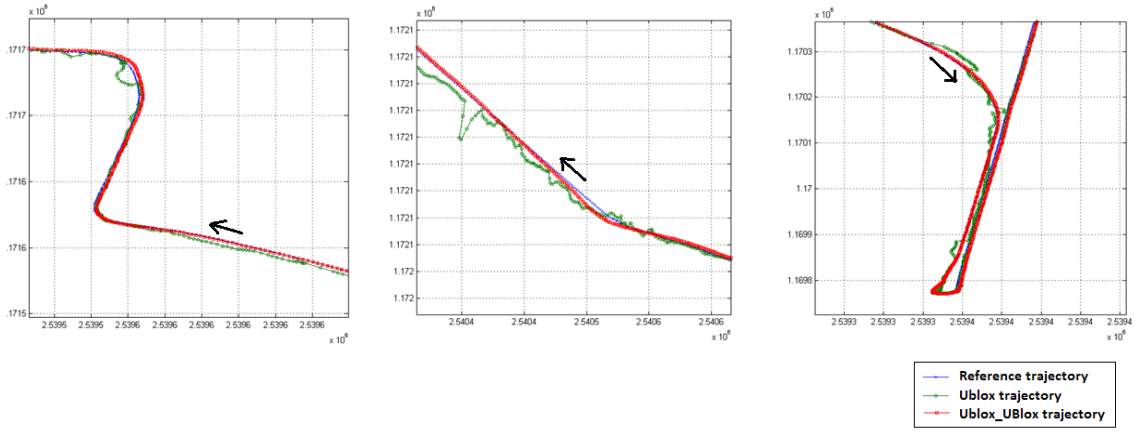

Figure 13: Vehicle alignment overlays obtained for three driving sections for the Ublox-trj, Ublox_Ublox-trj and the Ref-trj.

The second part of the analysis examines the precision and reliability error budget obtained for the *Javad-trj* and the *Ublox-trj* trajectories and how these compare to each other. Figure 14 shows the along- and off-track precision and trueness estimates obtained for the *Javad-trj*. Perhaps the most important thing to note from Figure 14 is the fact that trueness (shown in blue) lies consistently within the boundary zone defined by the precision level (shown in red/green) of the solution, suggesting that the precision error describes realistically the position fixes. The reader has to bear in mind, that the represented values for the estimated error represent the 1σ boundary. Regarding the precision values, the rapid changes observed at certain trajectory sections may reflect the abrupt changes in the observation conditions. For instance, the high uncertainty values observed for segments around 600 s and 900 s correspond to low satellite availability / high DOP values shown in Figure 7.

Similar conclusions are drawn for the *Ublox-trj* trajectory accuracy values shown in Figure 15. As expected, the *Ublox-trj* solution results in marginally higher uncertainties, whereas trueness estimates seem noisier compared to the *Javad-trj* solution.

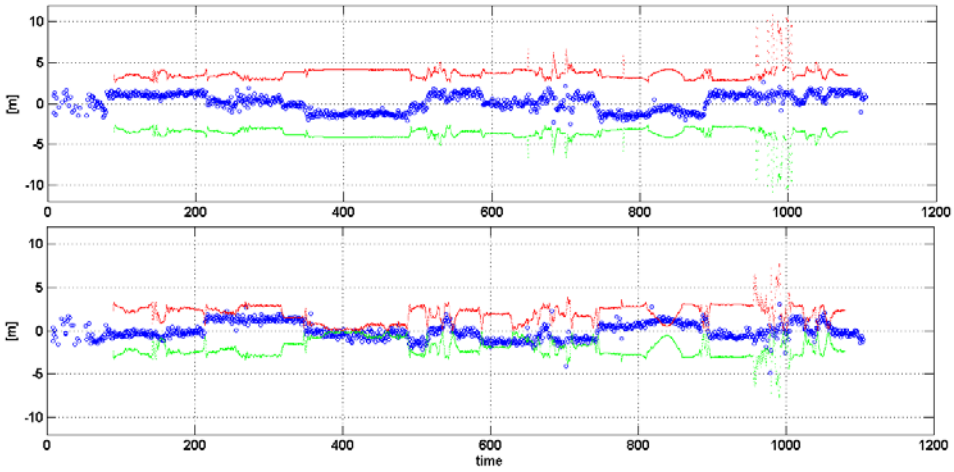

Figure 14: Along-track (top) and off-track (bottom) timeseries of 1-sigma precision (red-green) and trueness (blue) estimates obtained for the *Javad-trj*.

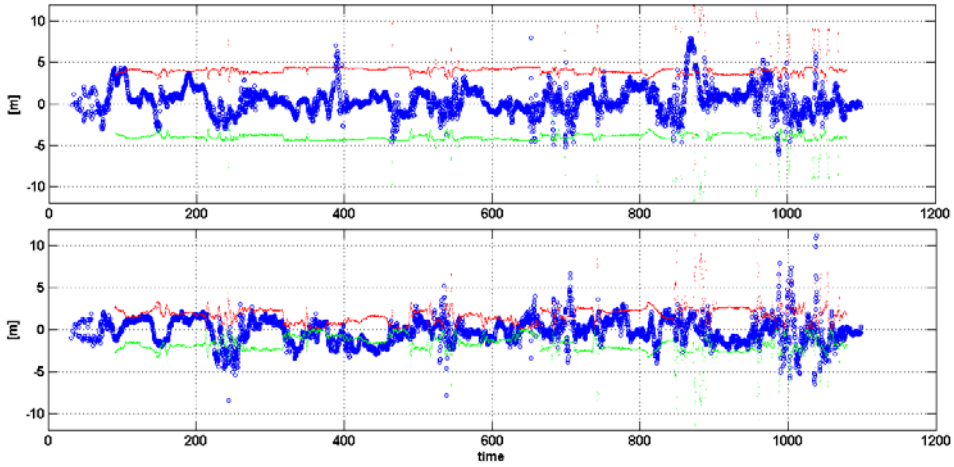

Figure 15: Along-track (top) and off-track (bottom) timeseries of 1-sigma precision (red-green) and trueness (blue) estimates obtained for the *Ublox-trj*.

As stated in Section 4.2.2, in addition to GNSS trajectory assessment a preliminary evaluation of the smartphone IMU sensors is attempted. The goal is to examine their potential to describe vehicle kinematics as part of different ITS application scenarios. In this article, two cases of clearly defined steep turns and a case of three successive turns are considered (see Fig. 16). All events correspond to a suburban environment driven at a maximal speed 30 km/h. Figure 17 shows the vehicle azimuth (orientation of the car with respect to the North-direction) computed using the reference trajectory solution as detailed in Section 5.2. In addition, it shows the *AirINS* (navigational grade INS) and *iPHONE 5S* y-acceleration and z-gyro values which correspond to the lateral acceleration and yaw rate respectively.

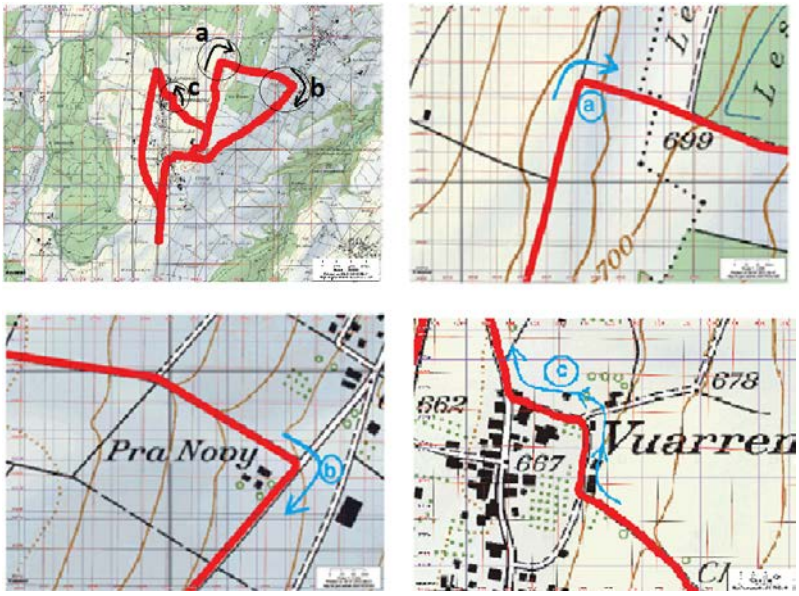

Figure 16: The three turning events used to study the iPhone 5S performances (© 2014 swisstopo (JD100064)).

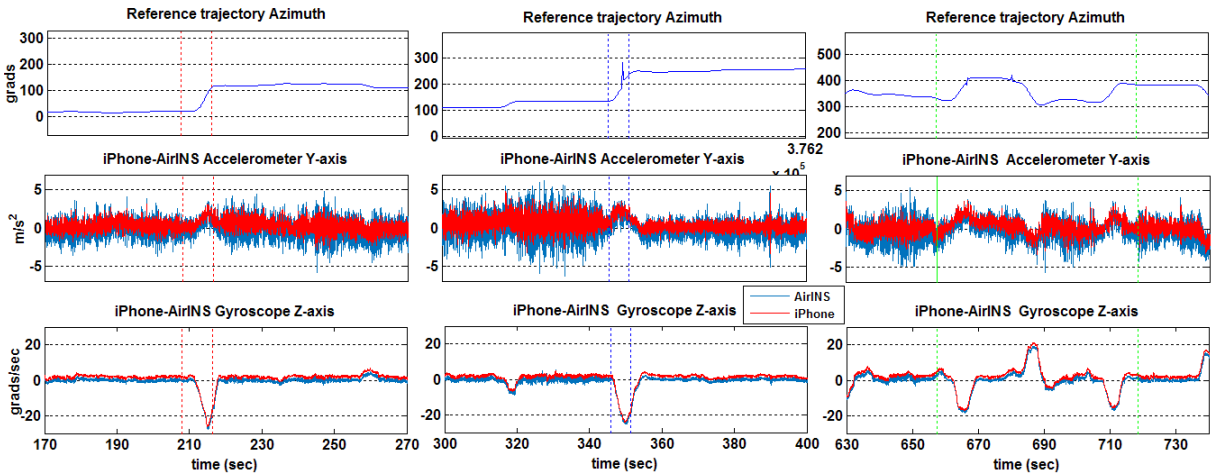

Figure 17: Computed azimuth (top), AirINS and iPhone 5S acceleration (middle) and gyroscope (bottom) timeseries obtained for the three maneuvering events a-b-c shown in Figure 16.

From Figure 17 it is apparent that the smartphone detected clearly all three events. Specifically, the changes in the z-gyroscope (bottom) indicate the changes in vehicle orientation and agree with those in azimuth (top) both in sign and magnitude. The results of vehicle lateral acceleration (middle), as expected indicate a transient increase as a result of the turn. The significantly lower sampling frequency of the *IPhone*-data let it seem, as if it were less "noisy" than the data from the *AirINS* which is sampled at a much higher frequency. But it is just an effect from the representation.

6 Implications of GNSS Performance Capabilities on ITS applications

The use of different positioning datasets, recorded under variable environmental conditions, has shown that there is no universal procedure for the assessment of accuracy. The question is the following: "*Is the achieved accuracy of positioning system (low cost) adequate for its use in ITS?*". This question although straightforward and fully justified does not have a simple answer. ITS and their operations range from comfort systems to safety-critical ones, hence different types of solutions require different levels of positioning performance. Positioning accuracy requirements mainly depend on the level of detail (which road, which lane, where on the lane) that a vehicle localization is estimated. Several research efforts have provided rough accuracy requirements which are 5 m, 1.1-1.5 m and 0.5-1.0 m respectively (Stephenson et al., 2011, Austroads Research Report, 2013), however, no specific requirements have been set for specific ITS applications. The main focus of this field experiment was the assessment of positioning accuracy. One must take into account other quality indicators, like availability and continuity, which are relevant for the performance evaluation of a positioning terminal (Capelle, 2014).

ITS can be classified in specific categories based on several characteristics. Examples include the type of "support" they provide (e.g. support to the driving task, information, monitoring), the driving conditions when the system operates in respect to a possible crash (e.g. normal driving/pre-crash systems, crash, post-crash), their human machine interface (HMI) (e.g. informative, warning, intervening), stand-alone systems vs. cooperative systems, and so on. Table 3 presents several ITS functions and their corresponding HMI.

Based on the presented range of ITS, it is evident that different systems require different positioning data to operate, as well as to have different requirements. In addition, specific types of data can be acquired either by GNSS or by other types of equipment that can be integrated in the vehicle. To exemplify the range of needs as well as the accuracy requirements for GNSS data one system will be described – namely, Intelligent Speed Adaptation (ISA).

ISA targets speeding, and its operation is as follows (Spyropoulou et al., 2014): the system monitors driver speed and compares it with a threshold value which is relevant to the posted speed limit. If the vehicle speed is over the threshold value the system informs the driver (informative), warns the driver (warning) or does not allow a driver to adapt the speed higher

than the threshold value (intervening). In terms of required data, the vehicle position is required to estimate its location and place in the respective road segment, which has a certain speed limit. The driver speed can be estimated either via GNSS data or by the vehicle's speedometer or a wheel counter.

Table 3: Classification of ITS for "normal driving" conditions.

Longitudinal Control	**Lateral Control**	**Collision Avoidance**	**Information**	**Monitoring**	**Perception**	**Comfort**
intelligent speed adaptation *inf, wrn, int*	lane departure *inf, wrn, int*	collision avoidance *inf, wrn, int*	navigation *inf*	fatigue *inf, wrn, int*	vision enhancement *inf*	e-toll
autonomous cruise control *int*	lane warning *inf, wrn, int*	obstacle warning *inf, wrn*	advanced navigation *inf*	vigilance *inf, wrn, int*	parking aid *wrn*	
automated highway systems *int*		intersection warning *inf, wrn, int*	real traffic information *inf*	alcolock *inf, wrn, int*		
			adverse conditions *inf, wrn*			
Crash Systems : smart restraints *int*						
Postcrash systems: ecall *int*						
* HMI: *inf*: information systems, *wrn*: warning systems, *int*: intervening systems						

Furthermore, the time is relevant only in cases where variable speed limits are implemented (dynamic speed limits that are not constant throughout the day). In this case, the vehicle speed at a certain time of the day has to be compared with the prevailing speed limit at the same time. The data accuracy is not that critical compared to other ITS, however, the requirement varies depending on road characteristics and system HMI. In cases, where different lanes have different speed limits (e.g. heavy occupancy vehicle lanes) the vehicle needs to be placed in the correct lane, rather than just the road segment, hence, higher accuracy is required to achieve robust lane detection. In terms of HMI interface, higher accuracy should be required with the intervening and warning system rather than the informative one (Gilliéron et al, 2005).

7 Conclusion

The deployment of very demanding location-based applications has to rely on a robust positioning platform which enables the integration of appropriate sensors, including GNSS. The technology is evolving rapidly and its specification has to be appropriate to the requirements of ITS services, which may differ from one application to another. The actual lack of standards and certification procedures for navigation terminals is one of the facts that motivate the creation of the SaPPART COST Action.

This paper presented one of the real contributions to the development of a methodology for the assessment of the positioning performance of the navigation terminal for road applications.

Providing valuable data sets of positioning data collected in real life scenarios has proven the variability of GNSS signals along a vehicle trajectory and the necessity to monitor continuously the positioning accuracy. This practical experiment is a first step for the definition of quality indicators which must fit the requirements of the challenging ITS application.

Acknowledgements

The authors gratefully acknowledge the SaPPART COST Action (TU 1302) for the funding of a short scientific mission to Lausanne (Switzerland) which allows young researchers to perform valuable navigation tests.
Research supported by the Action: ARISTEIA-II (Action's Beneficiary: General Secretariat for Research and Technology), co-financed by the European Union (European Social Fund – ESF) and Greek national funds.

References

1. Austroads Research Report (2013). *Vehicle positioning for C-ITS in Australia* (background document). AP-R431-13, Austroads Ltd, Sydney.
2. Capelle Y. (2014). *Performance management for GNSS based RUC systems*. Special interest session 13, ITS Europena Congress, Helsinki, June 2014.
3. Danezis, C. and Gikas, V. (2012). *An Iterative LiDAR DEM-aided Algorithm for GNSS Positioning in Obstructed/Rapidly Undulating Environments*. Advances in Space Research, Vol. 52, pp. 865-878.
4. Gillieron P-Y., Peyret F. SaPPART (2014). *Satellite Positioning Performance Assessment for Road Transport*, TRA.
5. Gilliéron P.-Y., Gontran H., Frank J. (2005),.*High quality road mapping for in-vehicle road safety*, European Navigation Conference GNSS 2005.
6. Groves P.D. *Principles of GNSS, Inertial, and Multisensor Integrated Navigation Systems*. Artech House, 2008.
7. ISO 5725-1:1994, Accuracy (trueness and precision) of measurement methods and results -- Part 1: General principles and definitions.
8. Kealy, A., Retscher, G., Alam, N., Hasnur-Rabiain, A., Toth, C., Grejner-Brzezinska, D. A., Moore, T., Hill, C., Gikas, V., Danezis, C., Bonenberg, L. and Roberts, G. W. (2012). *Collaborative Navigation with Ground Vehicles and Personal Navigators*. IEEE Xplore,

Proceedings of the 2012 International Conference on Indoor Positioning and Indoor Navigation (IPIN), Sydney, Australia, Nov. 13-15.

9. Musoff, H. and Zarchan, P. (2005). *Fundamentals of Kalman Filtering: A Practical Approach*, 3rd ed., American Institute of Aeronautics and Astronautics.

10. Retscher, G. and Kealy, A. (2006). *Ubiquitous Positioning Technologies for Modern Intelligent Navigation Systems*. Journal of Navigation, Vol. 59(01), pp. 91-103.

11. Spyropoulou, I., Karlaftis, M., Reed, N.(2014). *Intelligent Speed Adaptation and driving speed: Effects of different system HMI functionalities*, Transportation Research Part F: Traffic Psychology and Behaviour, Volume 24, May 2014, Pages 39-49.

12. Stebler Y., Guerrier S., Skaloud J., Victoria-Feser M.-P. (2011). *Improving Modelling of MEMS-IMUs Operating in GNSS-denied Conditions*. ION GNSS 2011, Portland, Oregon, USA, September 19-23, 2011.

13. Stebler Y., Skaloud J (dir.). (2013). *Modeling and Processing Approaches for Integrated Inertial Navigation*. EPFL thesis, n° 5601 (2013).

14. Stephenson, S., Meng, X., Moore, T., Baxendale, A., Edwards, T. (2011). *Accuracy Requirements and Benchmarking Position Solutions for Intelligent Transport Location Based Services*. Proceedings of the 8th International Symposium on Location-Based Services, 21-23 November, 2011, Vienna.

15. Waegli A., Schorderet A., Prongue C., Skaloud J. (2008). *Accurate trajectory and orientation of a motorcycle derived from low-cost satellite and inertial measurement systems*. ISEA 2008 Conference on Engineering of Sport 7, Biarritz, June 02-06, 2008.

16. http://www.berndthomas.net/berndthomas.net/SensorLog.html

17. http://www.ixblue.com/products/airins

18. http://www.swisstopo.ch

19. http://www.sappart.net